European Polymer Journal 95 (2017) 581–595

Contents lists available at ScienceDirect

European Polymer Journal

journal homepage: www.elsevier.com/locate/europolj

Sulfonated copolyimides containing trifluoromethyl and phosphine oxide moieties: Synergistic effect towards proton exchange membrane properties

Arun Kumar Mandal[a], Soumendu Bisoi[a], Susanta Banerjee[a,*], Hartmut Komber[b], Brigitte Voit[b]

[a] Materials Science Centre, Indian Institute of Technology Kharagpur, Kharagpur 721302, India
[b] Leibniz-Institut für Polymerforschung Dresden e.V., Hohe Strasse. 6, 01069 Dresden, Germany

ARTICLE INFO

Keywords:
Sulfonated copolyimides
Nuclear magnetic resonance (NMR)
Trifluoromethyl group
Phosphine oxide moiety
Proton conductivity
Oxidative stability

ABSTRACT

This paper reports the synthesis and characterization of a series of new semi-fluorinated sulfonated copolyimides (co-SPI) using a new trifluoromethyl and phosphine oxide containing diamine monomer, namely bis[4-(4′-aminophenoxy)-3-trifluoromethyl phenyl] phenylphosphine oxide (DFPPO). The copolymers were prepared by one pot polycondensation reaction of a mixture of two diamine monomers, namely 4,4′-diaminostilbene-2,2′-disulfonic acid (DSDSA) and DFPPO with the equimolar amount of 1,4,5,8-naphthalenetetracarboxylic dianhydride (NTDA). All these copolymers were soluble in several organic solvents and size exclusion chromatography indicated the formation of high molar masses. The membranes prepared from these copolymers by solution casting route showed good mechanical properties. The polymers were characterized by FTIR and NMR spectroscopic techniques that confirmed the polymer repeat unit structures. The degree of sulfonation of the copolymers was determined from ^{1}H NMR signal intensities. Transmission electron microscopy (TEM) and atomic force microscopy (AFM) images of the membranes showed phase separated morphology. In general, all the copolyimides showed high proton conductivity and reasonably high oxidative and hydrolytic stability. The co-SPI membrane DFPNH-90 (90% degree of sulfonation) with IEC_W = 2.86 mequiv g^{-1} showed proton conductivity as high as 237 mS cm^{-1} at 80 °C.

1. Introduction

The current rapid growth of technology, population and global warming caused by the fossil fuel sources is encouraging researcher to find alternative energy processes and sources. Among the different kind of energy devices, polymer electrolyte membrane (PEM) fuel cells have been widely considered as an automotive, portable and stationary power sources to reduce most of the problems associated with the production and consumption of energy [1–5]. PEM is a key component in these systems, which functions as an electrolyte for transferring protons from anode to cathode as well as providing a barrier to electrons and gas cross-leaks between the electrodes. Fuel cells provide pollution free operation, high energy conversion efficiency and low maintenance costs. In the present context, perfluorosulfonic acid (PFSA) ionomer membranes, e. g. Nafion®, Aciplex®, Flemion® are considered as state-of-the-art membrane for fuel cell applications due to their excellent chemical and physical stability along with high proton conductivity. However, difficult synthetic procedure, low glass transition temperature, restricted operation temperature (< 80 °C), and high fuel

* Corresponding author.
E-mail address: susanta@matsc.iitkgp.ernet.in (S. Banerjee).

http://dx.doi.org/10.1016/j.eurpolymj.2017.08.050
Received 22 June 2017; Received in revised form 18 August 2017; Accepted 30 August 2017
Available online 01 September 2017
0014-3057/

crossover limit their application. These have stimulated the activities to develop low-cost and high-performance new aromatic semifluorinated sulfonated polymers as alternative PEM materials. To develop alternate PEM materials, several classes of aromatic polymers such as sulfonated poly(arylene ether)s (SPAEs) [6], sulfonated polyimides (SPIs) [7–9], sulfonated poly(arylene ether sulfone)s (SPAESs) [10,11] and sulfonated polytriazoles (SPTAs) [12] were synthesized and their properties have been investigated.

Among the different classes of sulfonated polymers, sulfonated polyimides membranes are one of the potential candidates for PEM application, due to their high thermal, chemical and mechanical stability, excellent film forming ability, strong resistance to fuel crossover and high proton conductivity [13,14]. The first generation sulfonated polyimides derived from five-membered anhydrides were generally unstable towards acid due to the ease of hydrolysis of the imide linkages. The second generation sulfonated polyimides were derived from six-member ring containing naphthalenetetracarboxylic dianhydride (NTDA) showed improved performance as proton exchange membranes [15]. Due to the lower ring strain, six membered polyimides have superior chemical and thermal stability compared to the more common five-membered polyimides [16]. However, many of the six membered polyimides showed poor solubility in organic solvents and their high softening temperatures restricted many of the practical applications. Many research groups have incorporated flexible ether linkages in the polymer backbone for the improvement of solubility along with chemical and dimensional stability of the polyimides [14]. The oxidative stability of the PEM is an important consideration for their practical application in fuel cells. In recent years, Watanabe et al. reported that introduction of phenylphosphine oxide moiety in the polymer backbone enhances oxidative stability as well as proton conductivity [17]. Furthermore, phenylphosphine oxide moiety provides excellent adhesive properties with the catalyst layer [18]. Fluorinated polymers are of special interest because the incorporation of fluorine improves many of the polymer properties [19–21]. The trifluoromethyl groups in the polymers increase the electron density of the carbonyl carbon of imide groups and resist it to attack from peroxide radicals [22].

The water uptake and swelling ratio of the PEMs are also vital factors for fuel cell performances. A high water uptake and swelling ratio increase fuel crossover and deteriorate the mechanical properties of PEMs. Therefore, the optimization of the polymer structure is required to achieve high proton conductivity, low fuel permeability, high hydrolytic and oxidative stability for useful applications. In our previous work, several sulfonated polyimides were prepared using the phosphine oxide diamine monomer, bis [4-(4′-aminophenoxy) phenyl] phenylphosphine oxide (DATPPO) [23] and the trifluoromethyl group containing diamine monomer, 1,4-bis[3′-trifluoromethyl-4′(4″-aminobenzoxy) benzyl] benzene (TA) [7,24], and their properties have been investigated. In general, the copolymers prepared using these monomers showed promising proton exchange membrane properties but still many of the properties could be improved. Especially, when DATPPO was used, it was not possible to prepare the copolymers with DS higher than 60 and that compromised the IEC of the copolymers. The copolymers with DS higher than 60 showed limited solubility in polymerization solvent.

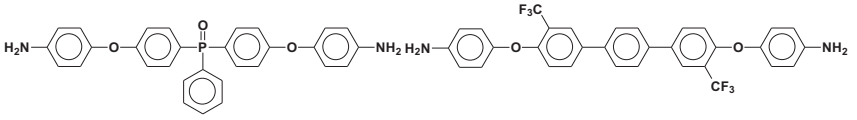

DATPPO TA

In this work, to utilize the best properties of both phosphine oxide and trifluoromethyl groups, a new diamine monomer DFPPO was designed and prepared. It is expected that polyimides prepared from this monomer should have improved solubility, oxidative stability, and hydrolytic stability.

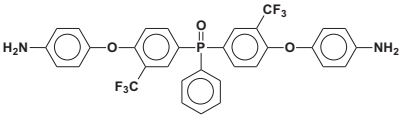

DFPPO

Accordingly, this work reports the synthesis and characterization of a series of new sulfonated copolyimides, where DFPPO has been used as one of the comonomers. The structures of the sulfonated polyimides named as DFPNH-XX [where XX represents the mole percent of sulfonated monomer, 4,4′-diaminostilbene-2,2′-disulfonic acid (DSDSA)] were characterized by NMR and FTIR spectroscopy. The membranes were prepared from these copolymers by solution casting method and their usefulness as PEM has been thoroughly investigated and compared with other structurally analogue polymers.

2. Experimental

2.1. Materials

1,4,5,8-Naphthalenetetracarboxylic dianhydride (NTDA, 98.0%) was purchased from TCI (USA) and dried under vacuum at 120 °C for 12 h prior to use. 4,4′-Diaminostilbene-2,2′-disulfonic acid (DSDSA, 95.0%) and Nafion® 117 membrane were purchased from Alfa Aesar (USA). The membrane was treated with hot 5 wt% H_2O_2 aqueous solution for 1 h followed by boiling 1 M H_2SO_4 aqueous solution for 1 h and washed several times with deionized water before use. Triethylamine (TEA, 99.0%), m-cresol (99.0%), benzoic acid (> 99.5%) and concentrated sulfuric acid (95%) were purchased from E. Merck (India) and were used as received. N, N-

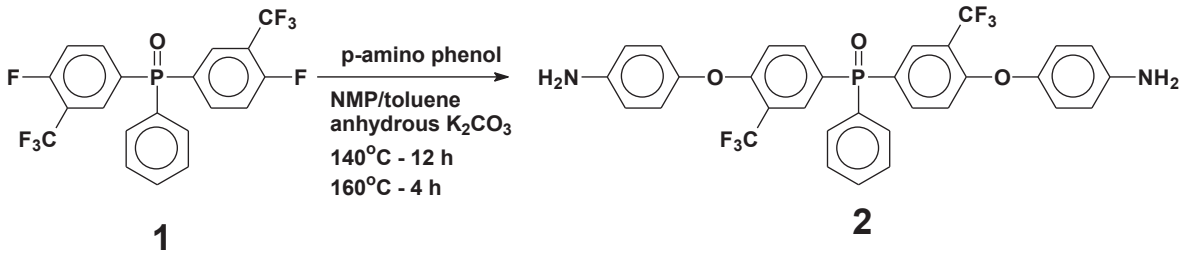

Scheme 1. Reaction scheme of synthesis of diamine monomer 2 (DFPPO).

Dimethylacetamide (DMAc), N,N-dimethylformamide (DMF), dimethyl sulfoxide (DMSO), N-methyl pyrrolidone (NMP), dichloromethane (DCM), acetone and isopropanol were purchased from Spectrochem (India) and were purified following the standard purification procedure. The compound bis [4-(4′-aminophenoxy)-3-trifluoromethyl phenyl] phenylphosphine oxide (2) was prepared according to Scheme 1. The monomer 1 was prepared according to the reported procedure [25].

2.2. Synthesis of bis [4-(4′-aminophenoxy)-3-trifluoromethyl phenyl] phenylphosphine oxide (2; DFPPO)

A 250 mL three neck round-bottom flask equipped with a mechanical stirrer, a nitrogen inlet and a Dean - Stark trap was charged with compound 1 (5 g, 0.011 mol), 4-aminophenol (3.03 g, 0.028 mol), potassium carbonate (9.59 g, 0.069 mol), NMP (40 mL) and toluene (25 mL). The reaction mixture was initially heated for 12 h at 140 °C and the water was (generated through the deprotonation of the phenol) removed by azeotropic distillation with toluene. After that, the temperature was increased to 160 °C and stirring was continued for another 4 h. The completion of the reaction was monitored by thin layer chromatography. Finally, the reaction mixture was cooled to room temperature and poured into large excess of water. The off-white precipitate was filtered and washed with distilled water for several times and dried under vacuum at 70 °C. The crude compound was purified by silica gel column chromatography using dichloromethane as eluent to get the diamine 2.

Yield: 5.6 g (~80%). Anal.Calcd.for $C_{32}H_{23}F_6N_2O_3P$ (628.5 g mol^{-1}): C, 61.15%; H, 3.69%; N, 4.46%; found: C, 61.02%; H, 3.62%, N, 4.35%.

FTIR (KBr, cm^{-1}): 3342, 3223 (N—H); 3047 (aromatic C—H stretching); 1195 (P═O); 1119 (ether linkage); 1052 (C—F stretching).

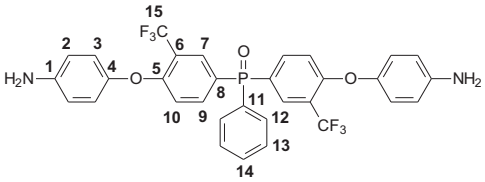

^{1}H NMR (DMSO-d_6, 30 °C): 7.89 (2H, dd, $^{3}J_{PH}$ = 11.6 Hz, $^{4}J_{HH}$ = 1.8 Hz; 7), 7.81 (2H, ddd, $^{3}J_{PH}$ = 8.7 Hz, $^{3}J_{HH}$ = 8.7 Hz, $^{4}J_{HH}$ = 1.8 Hz; 9), 7.7–7.6 (3H; 12, 14), 7.57 (2H, m; 13), 6.95 (2H, d, $^{3}J_{HH}$ = 8.7 Hz; 10), 6.84 (4H, d, $^{3}J_{HH}$ = 7.8 Hz; 2), 6.63 (4H, d, $^{3}J_{HH}$ = 7.8 Hz; 3), 5.15 ppm (4H, br; NH_2).

^{13}C NMR (DMSO-d_6, 30 °C): 160.0 (5), 146.8 (4), 143.6 (1), 137.8 (d, $^{2}J_{PC}$ = 11.3 Hz; 9), 132.6 (14), 131.8 (d, $^{1}J_{PC}$ = 106 Hz; 11), 131.5 (d, $^{2}J_{PC}$ = 10.1 Hz; 12), 130.3 (m; 7), 129.0 (d, $^{3}J_{PC}$ = 12.3 Hz; 13), 125.0 (d, $^{1}J_{PC}$ = 108 Hz; 8), 123.2 (q, $^{1}J_{CF}$ = 273 Hz, 15), 121.4 (2), 118.1 (dq, $^{3}J_{PC}$ = 13.3 Hz, $^{2}J_{CF}$ = 30.3 Hz; 6), 116.7 (d, $^{3}J_{PC}$ = 12.4 Hz; 10), 115.0 ppm (3).

^{19}F NMR (DMSO-d_6, 30 °C): −61.1 ppm (15).

^{31}P NMR (DMSO-d_6, 30 °C): 23.5 ppm.

2.3. Preparation of copolymers (DFPNH-XX)

The schematic representation of synthesis of the co-SPIs is presented in Scheme 2. As an representative, the polymerization procedure of DFPN-70 is described. DSDSA (0.362 g, 0.978 mmol), 6 mL m-cresol and TEA (0.208 g, 2.05 mmol) were added in a 50 mL 3-necked round bottomed flask equipped with a magnetic stirrer and N_2 inlet. The mixture was heated at 80 °C with continuously stirring for 4 h till DSDSA was completely dissolved. Then, DFPPO (0.263 g, 0.419 mmol), NTDA (0.374 g, 1.396 mmol), benzoic acid (0.52 g) and m-cresol (5 mL) were successively added into the reaction mixture. The reaction was continued for 16 h at 180 °C and finally the temperature was raised up to 200 °C for 3 h. After completion of the reaction, the reaction mixture was cooled and diluted by adding 5 mL m-cresol and the dark brown viscous solution was poured dropwise in large excess isopropanol under constant stirring. The fibrous polymer collected by filtration was washed several times with isopropanol and dried under vacuum at 130 °C for overnight. The polymer yield was ~99%.

^{1}H NMR (DMSO-d_6, 90 °C): 8.9–8.7 (3, several signals due to different NDI –centered triads), 8.39 (26), 8.06 (d; 11), 8.01 (13), 7.95 (21), 7.90 (24), 7.77 (16), 7.70 (18), 7.64 (17), 7.57 (6), 7.47 (25), 7.35 ppm (7, 14). Intensity ratios vary with composition.

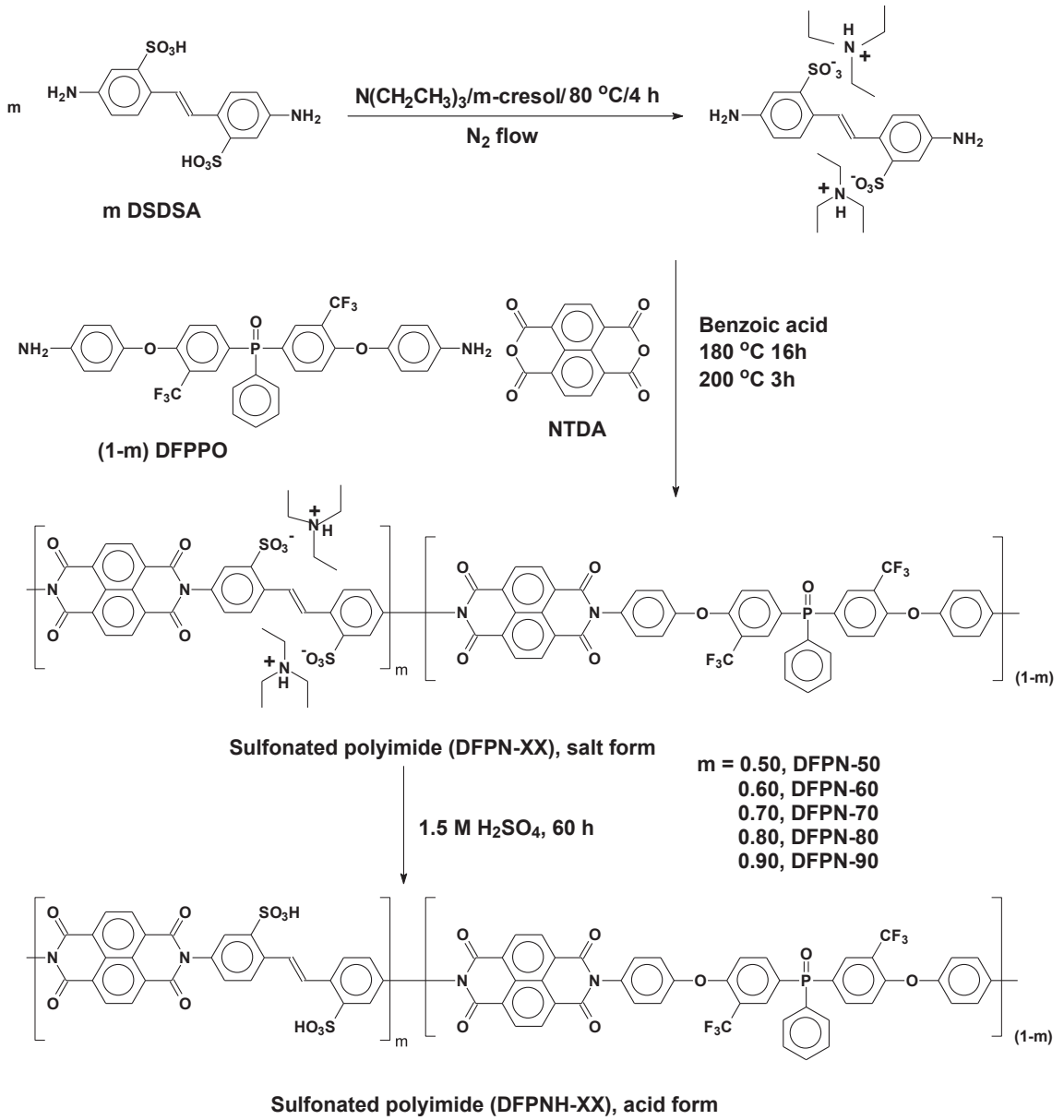

Scheme 2. Reaction scheme of synthesis of DFPNH-XX copolymers.

^{13}C NMR (DMSO-d_6, 60 °C): 162.9 and 162.8 (1), 157.7 (9), 154.6 (8), 146.2 (22), 138.1 (d, $^{2}J_{PC}$ = 10 Hz; 13), 135.3 (23), 133.7 (20), 132.7 (18), 132.2 (5), 131.5 (d, $^{2}J_{PC}$ = 9.9 Hz; 16), 131.3 (d, $^{1}J_{PC}$ = 106 Hz; 15), 131.2 (6), 130.5 (11), 130.4 (3), 129.5 (25), 129.0 (d, $^{3}J_{PC}$ = 13 Hz; 17), 128.2 (26), 127.8 (21), 127.1 (d, $^{1}J_{PC}$ = 108 Hz; 12), 127.5–126.5 (2, 4), 126.2 (24), 122.9 (q, $^{1}J_{CF}$ = 273 Hz; 19), 120.1 (m, 10), 120.0 (7), 119.3 ppm (d, $^{3}J_{PC}$ = 11.5 Hz; 14).

^{19}F NMR (DMSO-d_6, 90 °C): −60.6 ppm (19).

^{31}P NMR (DMSO-d_6, 90 °C): 23.3 ppm.

2.4. Film casting and acidification

The salt form of the copolymers was dissolved in DMSO with a concentration of 10% (w/v). The viscous polymer solutions were poured on flat bottom Petri dishes. The Petri dishes were heated at 80 °C for 24 h and then sequentially at 100 °C, 120 °C, 140 °C, 150 °C for 1 h at each temperature for controlled removal of the solvent. Finally, the Petri dishes were heated at 120 °C under vacuum for 24 h to remove any trace amount of solvent. The membranes were removed from the Petri dishes by putting them in boiling distilled water. The membranes in the salt form were converted to the acid form by treating them in 1.5 M sulfuric acid for 60 h, followed by rinsing with excess deionized water and finally drying under vacuum at 120 °C for 24 h. In all cases, yellowish-

transparent and flexible membranes were obtained with an average thickness of 51–59 μm.

2.5. Measurements

Attenuated total reflectance-fourier transform infrared (ATR-FTIR) spectra of the polymer membranes were recorded with Nexus 870 spectrometer in a humidity free atmosphere. ^{1}H (500.13 MHz), ^{19}F (470.59 MHz), ^{31}P (202.4 MHz) and ^{13}C (125.76 MHz) NMR spectra were recorded on an Avance III 500 NMR spectrometer (Bruker, Germany). To ensure full ^{1}H relaxation a pulse delay of 60 s was applied for the ^{1}H NMR measurements. DMSO-d_6 was used as solvent and internal reference (DMSO-d_6: $\delta(^{1}H) = 2.50$ ppm; $\delta(^{13}C) = 39.6$ ppm). The ^{19}F NMR spectra were referenced on external C_6F_6 ($\delta(^{19}F) = -163$ ppm) and the ^{31}P NMR spectra on external H_3PO_4 ($\delta(^{31}P) = 0$ ppm). The signal assignments were confirmed by ^{1}H-^{1}H and ^{1}H-^{13}C correlated spectra. The inherent viscosity (η_{inh}) of the polymers (0.5 g dL^{-1} polymer solution in NMP) was measured using an Ubbelohde suspended level viscometer at 30 °C. The molecular weight of the copolymers was determined by size-exclusion chromatography (SEC) using DMAc with 3 g L^{-1} LiCl as an eluent at a rate of 1 mL min^{-1}. The apparatus consists of HPLC pump 1200 (Agilent Technologies), a Polar Gel-M column (300 x 7.5 mm), a refractive-index (RI) detector K-2301 (Knauer) and a MiniDAWN light scattering (LS) detector (Wyatt Technology). Thermal stability of the polymers was evaluated from thermogravimetric analysis (TGA) using TA Instruments TGA Q50 thermal analyzer under synthetic air (N_2:O_2 = 80:20) at a heating rate of 10 K/min. The densities of the membranes were measured using a Wallace High Precision Densimeter-X22B (UK) (isooctane displacement) at 30 °C. The mechanical properties of the membranes (10 mm × 25 mm) in their acid form were measured at 30 °C using a tensile testing machine from TINIUS OLSEN, UK (H5KS) at a speed of 5 mm/min. The acidified membranes were dried under vacuum at 100 °C for 10 h under vacuum and cooled to room temperature (30 °C) inside a desiccator before performing the mechanical tests and reported as mechanical properties in dry condition. The dry membranes were immersed in deionized water for 24 h and wiped out any surface water using tissue paper and the mechanical properties reported as in wet condition. For each sample five test specimens were used. Transmission electron microscopy (TEM) of the membranes was performed using a TEM instrument, FEI -TECNAI G2 20 S TWIN. The samples in acid (H^+) form were stained with silver ion (Ag^+) by immersing them overnight in 0.5 M $AgNO_3$ aqueous solution followed by rinsing with water and dried at room temperature for 12 h. The stained membranes were embedded with epoxy resin and sectioned to yield 100 mm thick (using a Leica Ultracut UCT EM FCS, Austria) and placed on copper grids. The atomic force microscope (AFM) analysis was done using AFM 5500 (Agilent Technology) in tapping mode. The in-plane proton conductivity of the polymer membranes were determined using 4-probe conductivity cell using AC impedance spectroscopic technique. A sample of the rehydrated membrane of dimension 2 cm × 1 cm was clamped between two platinum electrodes in the conductivity cell. The membranes between the two electrodes was exposed to allow its equilibrium with deionized water during the experiment. The cell was attached to a Gamry Reference 3000 potentiostat/galvanostat/ZAR instrument. Resistance values (R) were determined from the impedance plot (Nyquist type plot) obtained in the frequency range of 100 Hz–1 MHz. The proton conductivity (σ) was calculated from the equation, $\sigma = L/(A \times R)$ where A and L are the conducting area and the membrane length, respectively.

The concentration of the ion conducting units is usually represented as the molar equivalents of ion conductor per mass of dry membrane and is expressed as weight based ion exchange capacity (IEC_w), or mill equivalents of ion per gram (equiv. g^{-1} or mmol g^{-1}) of polymer ($EW = 1000/IEC_w$). The ion exchange capacity for di-sulfonated copolymers was calculated from the following relationship (1):

$$IEC_w = (1000/MW_{repeat\ unit}) \times DS_{theo} \times 2 \quad (1)$$

where DS_{theo} is the degree of sulfonation (DS) calculated through monomer feed ratio; it can be defined as the mole fraction sulfonated monomer. The ion exchange capacities (IECw) of the membranes were determined by back-titration method as reported elsewhere [26]. IEC_W values were also derived from composition data determined by ^{1}H NMR spectroscopy. Water uptake and swelling ratio of the membranes in deionized water were measured at 30 °C and 80 °C for 3 days following the reported procedure [7,10]. Volumetric ion exchange capacity (IEC_V) values for both dry and wet state of the membranes were calculated by multiplying the density of the films with IEC_W and by taking account of the water uptake of the membranes respectively. The oxidative stability of co-SPIs was tested by immersing the films (10 mm × 10 mm) into immediately prepared Fenton's reagent (2 ppm $FeSO_4$ in 3% H_2O_2) at 80 °C. Hydrolytic stability was measured by immersing the membranes (10 mm × 10 mm) in deionized water at 80 °C for 24 h, the weight loss of the membranes was calculated and reported as% of weight loss in 24 h [23].

3. Results and discussion

3.1. Characterization of the polymers

A new semifluorinated diamine monomer (DFPPO) with phosphine oxide moiety was synthesized with high yield (~ 80%) as shown in Scheme 1. The compound was purified by column chromatography and was well characterized by FTIR and NMR spectroscopic techniques.

The sulfonated copolymers (co-SPIs) were synthesized by single pot high temperature solution imidization of poly(amic acid)s that were generated by the reaction of an equimolar amount of NTDA with a mixture of two diamine monomers (DFPPO and DSDSA), using benzoic acid as catalyst and m-cresol as solvent (Scheme 2). The DS of the copolymers was controlled by varying the molar ratio of the DFPPO to DSDSA (XX = mole percentage of sulfonated amine monomer, DSDSA). During the course of the reaction, the viscosity of the reaction medium increased dramatically. At the end of the reaction, the highly viscous solution was diluted with m-

Table 1
Properties of DFPNH-XX copolymers.

Polymer	η_{inh}[a] (dL/g)	M_w[b]	DS	
			Theo.[c]	NMR[d]
DFPNH-50	1.30	354000	0.50	0.47
DFPNH-60	1.02	288000	0.60	0.57
DFPNH-70	1.20	317000	0.70	0.65
DFPNH-80	0.92	171000	0.80	0.75
DFPNH-90	0.98	–	0.90	0.84

[a] η_{inh}, inherent viscosity in NMP at 30 °C.
[b] M_w, weight average molecular weight from SEC with LS detection.
[c] Theoretically calculated from the monomer feed ratio.
[d] Calculated from ^{1}H NMR signal intensities.

cresol and fibrous polymers were collected by precipitation in a large excess of isopropanol. The solubility behavior of the co-SPIs was checked in several organic solvents at a concentration of ~10% (w/v) at 30 °C. All the polymers were fairly soluble in polar aprotic solvents such as NMP, DMF, DMAc and DMSO and were insoluble in THF, DCM, methanol and water even at elevated temperatures. It was also noted that the co-SPIs in the form of TEA-salt showed good solubility in m-cresol, but not in their protonated form. The better solubility of the co-SPIs was due to the synergistic effects of the ether linkages (−O−), the bulky trifluoromethyl (−CF_3) and phosphine oxide groups present in the polymer backbone [19,20]. The ether linkages help in building different intrasegmental configurations and the CF_3 groups disrupt the regularity of the molecular chains and hindered the dense chain stacking, thereby improving the solubility [9]. Because of better solubility of these co-SPIs, it was possible to prepare copolymers with higher DS values in comparison to the earlier work [23]. The weight average molecular weight of the polymers was measured by the light scattering method and the values are reported in Table 1. The inherent viscosity of the co-SPIs reported in Table 1 is also indicating the formation of high molecular mass polymers. The membranes were prepared from the polymers from their salt form by solution casting method using DMSO as solvent and the salt forms of the membranes were converted to their corresponding acid forms by acid treatment.

The chemical structure of the copolymers was confirmed by both ATR-FTIR and NMR spectroscopy. In ATR-FTIR spectra (Fig. 1), the absorption bands of naphthalene imide rings appeared at 1670 cm^{-1} (−C═O symmetric stretching), 1714 cm^{-1} (−C═O asymmetric stretching) and 1343 cm^{-1}(−C−N asymmetric stretching) confirming the formation of the imide ring for all DFPNH-XX copolymers [7,23]. There were no 6-membered anhydride bands at 1770 and 1743 cm^{-1} and no characteristic peak of poly(amic acid) around 1780 cm^{-1}, demonstrating complete imidization. The absorption band at 1195 cm^{-1} indicating the presence of P═O functionality. The stretching frequency of C−F was observed at 1047 cm^{-1} and two SO_2 stretching vibrations of the sulfonic acid group were observed at 1078 cm^{-1} and 1013 cm^{-1}.

Detailed structural elucidation of the polymers was carried out by different NMR techniques. NMR spectroscopy allows access to the polymer structure by four different nuclei (Fig. 2). ^{19}F and ^{31}P NMR spectra prove that under polymerization conditions, both the CF_3 group and the triarylphosphine oxide moiety were non-reactive. The polycondensation reaction, which first results in a poly(amic acid), was completed to the polyimide as there was no sign of amide protons in the ^{1}H NMR spectrum of the polymers. Typical for sulfonated polyimides [7] but also polytriazoles of similar structure [12], there was a signal broadening resulting from restricted chain mobility most probably due to hydrogen bond formation. To a certain extent this can be reduced by high-temperature measurements (e.g. 90 °C for ^{1}H). The naphthalene diimide (NDI) central unit showed two symmetric triads (DFPPO - NDI - DFPPO and

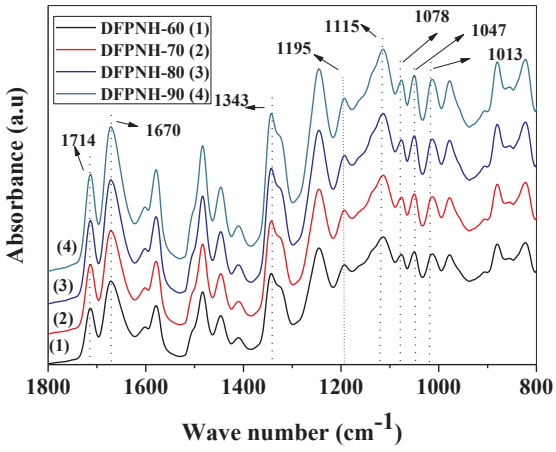

Fig. 1. ATR-FTIR spectra of DFPNH-XX copolymer membranes.

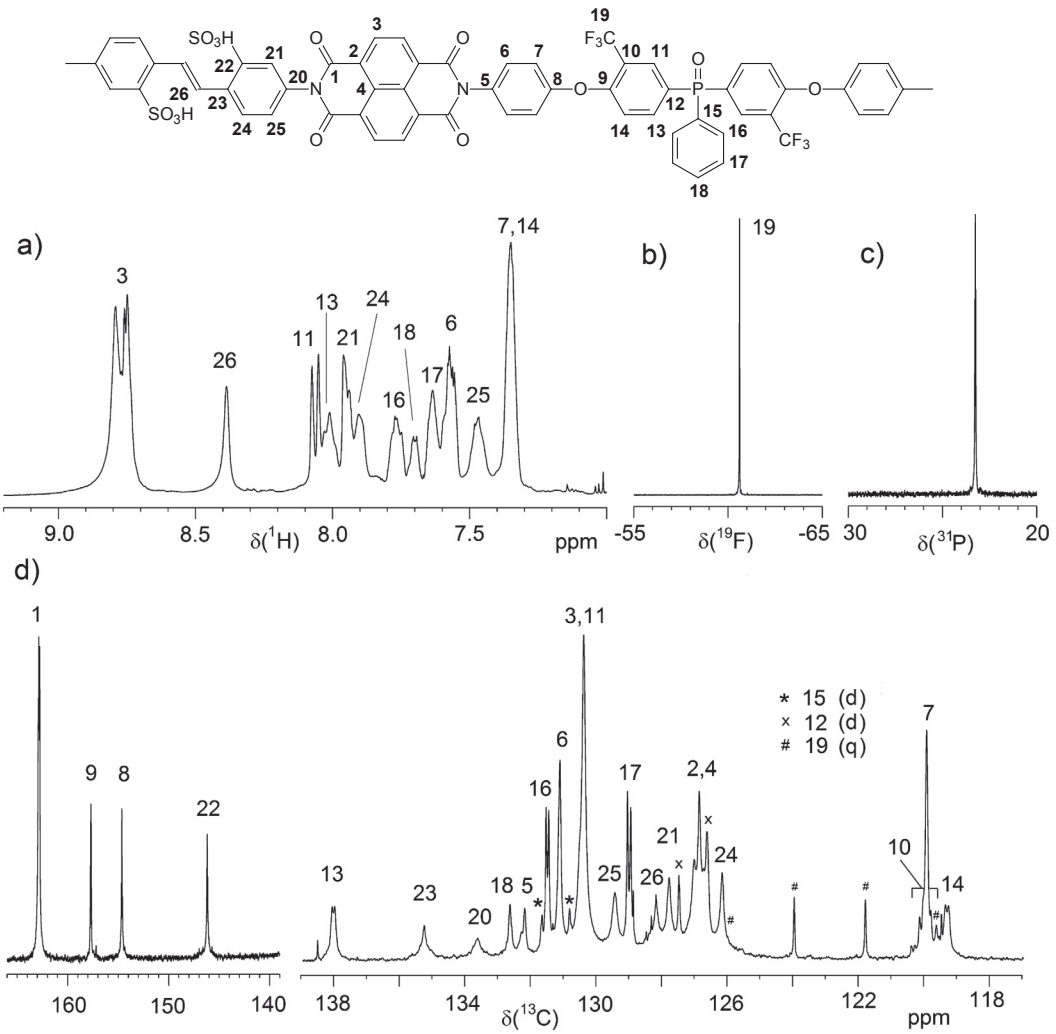

Fig. 2. Compilation of the ^{1}H (a), ^{19}F (b), ^{31}P (c) and ^{13}C (d) NMR spectra of DFPNH-60 copolymer (DMSO-d_6 at 90 °C, ^{13}C NMR at 60 °C). Multiplets resulting from $^{1}J_{PC}$ coupling are marked with different symbols in the ^{13}C NMR spectrum. Atom numbering according the given structural fragment.

DSDSA - NDI - DSDSA) and a non-symmetric one (DFPPO - NDI - DSDSA), which results in signal splitting for the NDI proton H_3. The complete ^{1}H and ^{13}C signal assignment, based also on 2D NMR spectra (Fig. 3), confirms the suggested polyimide structure (Fig. 2a,d). Several signals show the expected scalar couplings to ^{19}F and ^{31}P nuclei, respectively. Advantageously for quantification, one well separated signal appears for each subunit in the ^{1}H NMR spectra; this is H_3 for NDI, H_{26} for DSDSA and $H_{7,14}$ for DFPPO (Fig. 2a). The DS values given in Table 1 were calculated from the H_{26} and $H_{7,14}$ signal integral values.

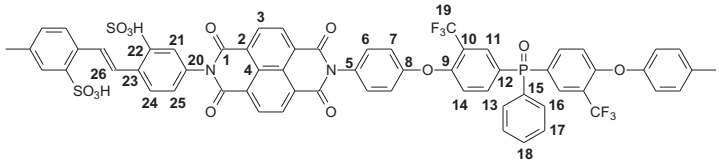

3.2. Thermal and mechanical properties

Thermal stability of the co-SPIs in acid form was investigated by thermogravimetric analysis (TGA) under synthetic air (Fig. 4). The copolymers were dried under vacuum at 120 °C before performing TGA to remove the absorbed water to the maximum extent to assess their actual thermal stability. Still, some of the TGA thermograms showed a small weight loss around 120 °C. This may be due to the loss of the residual high boiling solvent. The polymers showed reasonably high thermal stability with a two step degradation behavior as expected for sulfonated polyimides [19,21]. The 10% weight loss temperatures of the copolymers are given in Table 2. The values are indicating that the copolymers have reasonably high thermal stability (> 300 °C) that are required for PEM

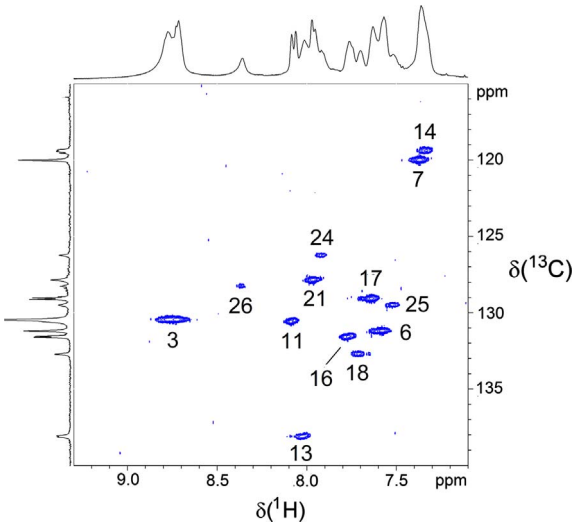

Fig. 3. ^{1}H-^{13}C heteronuclear single quantum coherence (HSQC) spectrum of DFPNH-60 copolymer (DMSO-d_6, 60 °C). The ^{1}H NMR spectrum is plotted along x-axis and the DEPT-135 spectrum is plotted along y-axis.

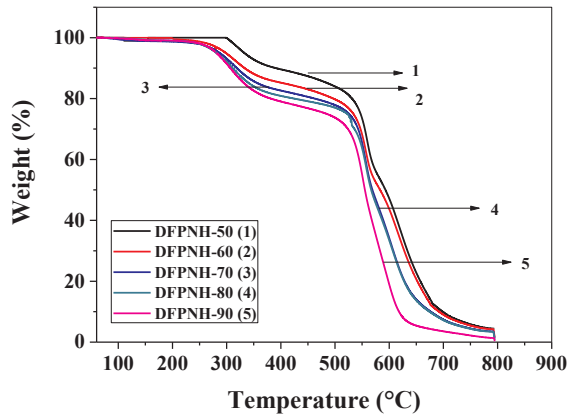

Fig. 4. TGA thermograms of DFPNH-XX copolymer membranes under synthetic air.

Table 2
Thermal and mechanical properties of DFPNH-XX polymers.

Polymer	$T_{d,\ 10}$[a] (°C)	Tensile strength (MPa)		Young's modulus (GPa)		Elongation at break (%)	
		Dry	Wet	Dry	Wet	Dry	Wet
DFPNH-50	370	90 ± 3	69 ± 2	2.35 ± 0.01	1.76 ± 0.02	16 ± 1.1	18 ± 1.9
DFPNH-60	330	77 ± 2	59 ± 4	2.10 ± 0.03	1.51 ± 0.04	14 ± 1.3	17 ± 1.8
DFPNH-70	314	70 ± 2	54 ± 3	1.79 ± 0.01	1.46 ± 0.03	12 ± 1.4	15 ± 1.1
DFPNH-80	309	57 ± 1	45 ± 3	1.73 ± 0.02	1.42 ± 0.02	10 ± 0.8	12 ± 1.5
DFPNH-90	301	51 ± 2	40 ± 2	1.55 ± 0.02	1.23 ± 0.01	8 ± 0.5	10 ± 1.1
Nafion® 117	–	38 ± 2	22 ± 1	0.26 ± 0.01	0.16 ± 0.02	288 ± 3.2	301 ± 3.8

[a] Degradation temperature corresponding to 10% weight loss, measured by TGA at a heating rate of 10 °C min^{-1} under synthetic air (N_2:O_2 = 80:20.

application [1,2]. As usual characteristic of the sulfonated polymers, the copolymers did not show any glass transition (T_g) in the temperature range of 30 °C to 350 °C in DSC. This is attributed to the strong ionic interactions of the sulfonic acid groups and presence of rigid triphenylphosphine oxide moiety and naphthalene groups in the polymer backbone [7,23].

Mechanical stability of PEMs under humidified working conditions is very important for their use in fuel cells. The stress-strain plots of the dry and hydrated membranes are shown in Fig. 5(a) and (b), respectively. The mechanical properties of the co-SPIs membranes are summarized in Table 2.

The DFPNH-XX membranes showed tensile strength in the range 51–90 MPa (dry state) and 40–69 MPa (hydrated state) which are considerably higher than that of Nafion® 117 [38 MPa (dry state) and 22 MPa (hydrated state)]. Therefore, the DFPNH-XX

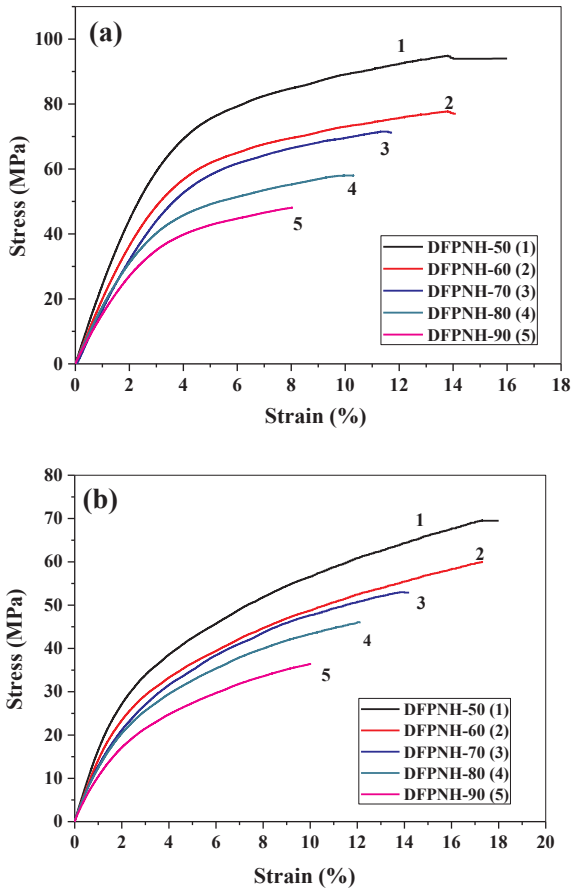

Fig. 5. Stress-strain plots of the DFPNH-XX copolymer membranes (a) in dry state and (b) in wet state.

copolymer membranes are durable enough for their application as PEM. The Young's modulus of the copolymers was in the range of 1.55–2.35 GPa (dry state) and 1.23–1.76 GPa (hydrated state), much higher than that of Nafion® 117 membrane (0.26 and 0.16 GPa for dry and hydrated states respectively). However, the elongation at break of the co-SPI membranes were in the range of 8–16% (dry state) and 10–18% (hydrated state) which were much lower compared to the Nafion® 117 m (~300%). This is a general characteristic of rigid co-SPIs compared to the polymers with soft fluorocarbon backbone [7,9,23]. However, it can be noted that there was no drop of the elongation at break of the co-SPIs in their hydrated state, rather it improves to some extent and the values are sufficient for the fabrication of membrane electrode assembly [1,9].

3.3. Ion exchange capacity and water uptake

The amount of exchangeable protons present in the acid form of the ionomer membranes is expressed as ion exchange capacity (IEC_w). It has a vital role in various PEM properties such as the water uptake, proton conductivity, etc. Theoretical IEC_w was calculated from the monomer feed ratio and the experimental IEC_W was calculated from the DS as obtained from ^1H NMR analysis and titrimetric measurements. The IEC_w values of co-SPI membranes are tabulated in Table 3. The theoretical IEC_w values were within the range 1.36 to 2.86 mequiv/g. IEC_w values, calculated from the polymer composition determined by ^1H NMR spectroscopy were in agreement with the theoretical values and the values are within the experimental error. Therefore, it can be stated that the sulfonic acid monomer (DSDSA) was quantitatively incorporated into the polymer backbone during the polymerization reaction [16].

Water uptake is another crucial property in PEMFC applications as it greatly influences the mechanical integrity and dimensional stability of the PEMs in their hydrated state. As a matter of fact, excessive water absorption may deteriorate the mechanical and dimensional stability [9]. At the same time, the membrane should absorb a reasonable amount of water as the water molecules dissociate the acid functionalities and facilitate proton transport by forming interconnected channels. This provides a better proton transport pathway and eventually increased proton conductivity in the PEM [27,28]. Therefore, trade-off relationship between water uptake and mechanical-dimensional stability is a challenge in the design of the right polymer membrane for PEM application. In the present investigation, the non-sulfonated monomer (**2, DFPPO**) plays a crucial role in controlling the water uptake values of these co-SPIs. This monomer was specially designed by incorporating additional $-CF_3$ groups in comparison to the previously reported phosphine oxide containing diamine monomer **DATPPO** [23]. Though, this structural manipulation of the diamine monomer resulted

Table 3
Density, IEC, water uptake and hydration number of DFPNH-XX membranes.

Polymer	d_M[a] (g/cm^3)	IEC_w (mequiv/g)			IEC_v[e] (mequiv/g))		Water uptake (wt%)[f]		Water uptake (vol%)[g]		λ[h] [H_2O/SO_3]	
		Theo[b]	Titr[c]	NMR[d]	Dry	Wet	30 °C	80 °C	30 °C	80 °C	30 °C	80 °C
DFPNH-50	1.29	1.36	1.30	1.27	1.70	1.42	20	23	26	30	8.4	9.7
DFPNH-60	1.27	1.70	1.65	1.60	2.16	1.68	28	32	35	41	9.1	10.7
DFPNH-70	1.28	2.05	1.95	1.88	2.62	1.88	40	47	51	60	10.8	12.7
DFPNH-80	1.31	2.44	2.30	2.25	3.20	2.10	52	60	68	78	11.8	13.6
DFPNH-90	1.13	2.86	2.62	2.53	3.23	2.00	61	70	69	79	11.9	13.6
TPPO-60[i]	1.28	1.84	1.83	1.81	2.35	1.79	31	41	39	52	9.4	12.3

[a] Density of membranes.
[b] $IEC_{w,theo}$ = (1000/$MW_{repeat\ unit}$) × DS_{theo} × 2; DS_{theo} is calculated theoretically from monomer feed ratio.
[c] Determined by titration.
[d] $IEC_{w,NMR}$ = (1000/$MW_{repeat\ unit}$) × DS_{NMR} × 2, where DS_{NMR} is calculated from ^{1}H signal integrals.
[e] IEC_v(dry) = ($IEC_{w,\ theo}$ × d_M); IEC_v (wet) = (IEC_v (dry)/(1 + 0.01 WU)) at 30 °C.
[f] WU (wt%) = (W_w- W_d)/W_d × 100.
[g] WU (vol%) = ((W_w - W_d)/d_w)/(W_d/δ_m) × 100. (W_w and W_d are the weights of the wet and dry membranes, respectively; d_m and d_w is the density of the membrane in the dry state and density of water (l g cm^{-3}), respectively).
[h] λ = WU (wt%)/(100 × $IEC_{w,\ theo}$. × $M_{W,H2O}$), where M_W (H_2O) = 18 g/mol.
[i] Reference[23]

copolymers with lower IEC values at the same degree of sulfonation, but the hydrophobic CF_3 groups improve many other membrane properties. The water uptake values for this series of co-SPIs were lower compared to many other sulfonated polyimide membranes [7,18,23]. This was attributed to the presence of both $-CF_3$ and polar phosphine oxide moiety (that form hydrogen bond with the sulfonic acid groups) in these co-SPIs [18,23]. In-plane proton conductivity of PEM is directly related to the length of the specimen and independent of mass [29]. Therefore, a better insight on proton conductivity is obtained when IEC_v is considered rather than IEC_w. IEC_v values of the co-SPI membranes are presented in Table 3. It is the molar concentration of sulfonic acid groups per unit volume of the polymer film taking into account the absorbed water. $WU_{vol\%}$ values of the co-SPI membranes were plotted against IEC_v (dry and wet) and are shown in Fig. 6a and b. IEC_v dry and wet of the co-SPI membranes showed a similar trend both 30 and 80 °C, except for very high DS (DS ~ 90), indicating no abrupt swelling of the membranes at higher temperature and better water management by the membranes. With the increase in IEC, the hydration number (λ) of the co-SPI membranes increases steadily, but the values are lower in comparison to Nafion® (λ ~ 15) [15]. This is attributed to the high rigidity of the aromatic SPI backbone compared to the flexible fluorocarbon structure of Nafion® and the strong ionic interaction among sulfonic acid groups which restricts the free volume for water absorption surrounding the ionic $-SO_3H$ groups beyond a certain limit. However, the water uptake of the co-SPI corresponds to λ ~ 4–6 is considered enough for smooth transportation of protons via a vehicular mechanism (migration of hydronium ions) [30].

The dimensional change of these co-SPIs is reported in the Table 4. A gradual increase in dimensional change was observed for all the co-SPIs as the DS value increases. This is attributed to the increase in the content of the sulfonic acid groups in the membranes that enhance the ionic nature of the co-SPIs [19]. All these co-SPIs that displayed anisotropic membrane swelling where the dimensional change was greater in through-plane (thickness) than in plane (length) direction (Fig. 7). It is expected that smaller dimensional change in in-plane direction of the membrane is preferable for fabrication of high quality membrane electrode assembly [7].

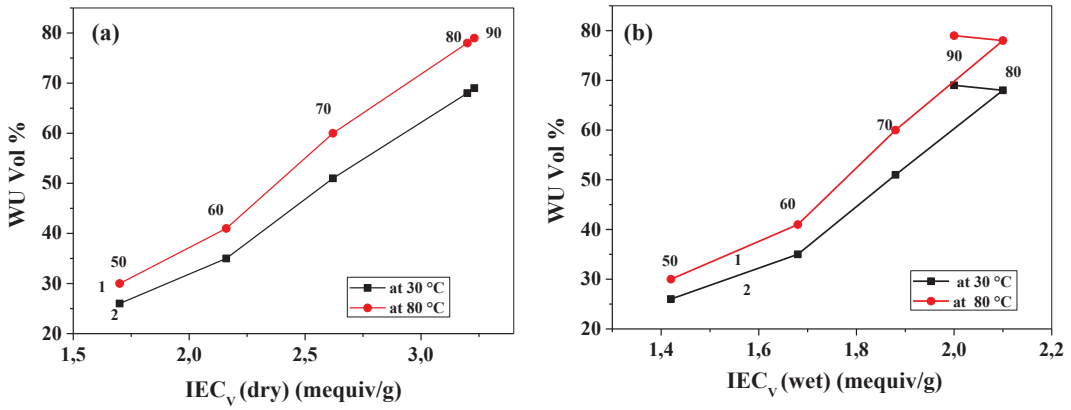

Fig. 6. Water uptake (vol%) dependence of (a) IEC_v (dry) and (b) IEC_v (wet) values of DFPNH-XX copolymer membranes.

Table 4
Swelling ratio, oxidative and hydrolytic stability of DFPNH-XX membranes.

Polymers	IEC_w (mequivg^{-1})	Thickness (μm)	Oxidative stability (h)		Hydrolytic stability[c] (%)	Swelling Ratio (%)			
			τ_1[a]	τ_2[b]		30 °C		80 °C	
						In plane	Through plane	In plane	Through plane
DFPNH-50	1.36	51	15	> 24	< 1	2.6	6.0	5.3	11.0
DFPNH-60	1.70	56	12	> 24	< 1	4.5	11.0	7.5	16.0
DFPNH-70	2.05	57	5	> 16	~1	6.0	15.0	9.0	23.0
DFPNH-80	2.44	59	3	> 9	4.0	8.0	21.0	11.0	27.0
DFPNH-90	2.86	58	1	> 2	6.0	10.0	25.0	14.0	30.0
p-DTN-70[d]	2.1	45	–	9	2.0	2	12	–	–
DTN-60[e]	2.13	48	–	1.4	–	1	15	–	–
TPPO-60[f]	1.84	36	3.1	20	5	5	5.5	10	13.8

[a] Time required to start breaking the membranes in 3% H_2O_2, 2 ppm $FeSO_4$ at 80 °C.
[b] Time required for the membranes to dissolve completely in 3% H_2O_2, 2 ppm $FeSO_4$ at 80 °C.
[c] Percentage weight loss of the membrane at 80 °C in 24 h.
[d] Reference [24].
[e] Reference [31].
[f] Reference [23].

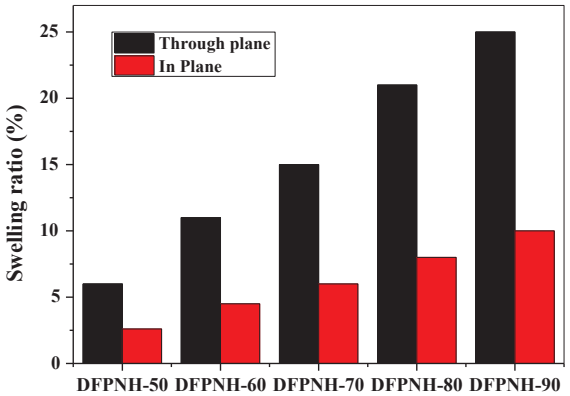

Fig. 7. Dimensional swelling of DFPNH-XX copolymer membranes at 30 °C.

3.4. Oxidative and hydrolytic stability

The oxidative stability is a measure of robustness of the membranes used in PEMFC. The oxidative and hydrolytic stability of DFPNH-XX membranes are tabulated in Table 4. The oxidative stability of the sulfonated copolymers decreases with increase in DS due to the increase in sulfonated sites in the membranes that are much more susceptible towards oxidative attack by hydroperoxy and hydroxy radical species (HOO· and HO·) [7,9]. In general, the copolymers of this series showed higher oxidative stability than many other sulfonated polyimides with similar IEC values [23,24,31]. It can be seen from Table 4 that DFPNH-70 has higher oxidative stability compared to p-DTN-70 (derived from TA, DSDSA and NTDA), DTN-60 and TPPO-60 prepared from the nonfluorinated diamine monomers. This can be attributed to the presence of both phosphine oxide and $-CF_3$ groups in the present series of co-SPIs that have a synergistic effect towards the oxidative stability of the membranes. Both these groups have the capability to stabilize free radicals generated by Fenton's reagent and prevent further degradation of the polymer chain [9,23]. As expected, the hydrolytic stability of the copolymers decreases with the increase in DS. However, the co-SPI membranes showed higher hydrolytic stability than analogous sulfonated copolymers reported earlier without $-CF_3$ groups [23]. Although, the oxidative and hydrolytic stability of these copolymers were lower than Nafion®, the membranes showed considerable improvement on these properties in comparison to the previously reported NTDA based polyimide membranes [7,23,24,31].

3.5. Copolymer microstructure

The microstructure of the membranes plays an important role in the proton transport mechanism. The surface morphology of the co-SPI membranes were examined by atomic force microscopy (AFM) in tapping mode of 10 μm × 10 μm membranes under ambient conditions (Fig. 8). In the AFM height images, there are two regions, one is bright and another is dark. As the degree of sulphonation increases, the area of bright region decreases and average roughness of the membrane decreases. The dark regions can be attributed to a soft structure (hydrophilic sulfonic acid groups) whereas the bright regions relates to the hard structure (hydrophobic polymer

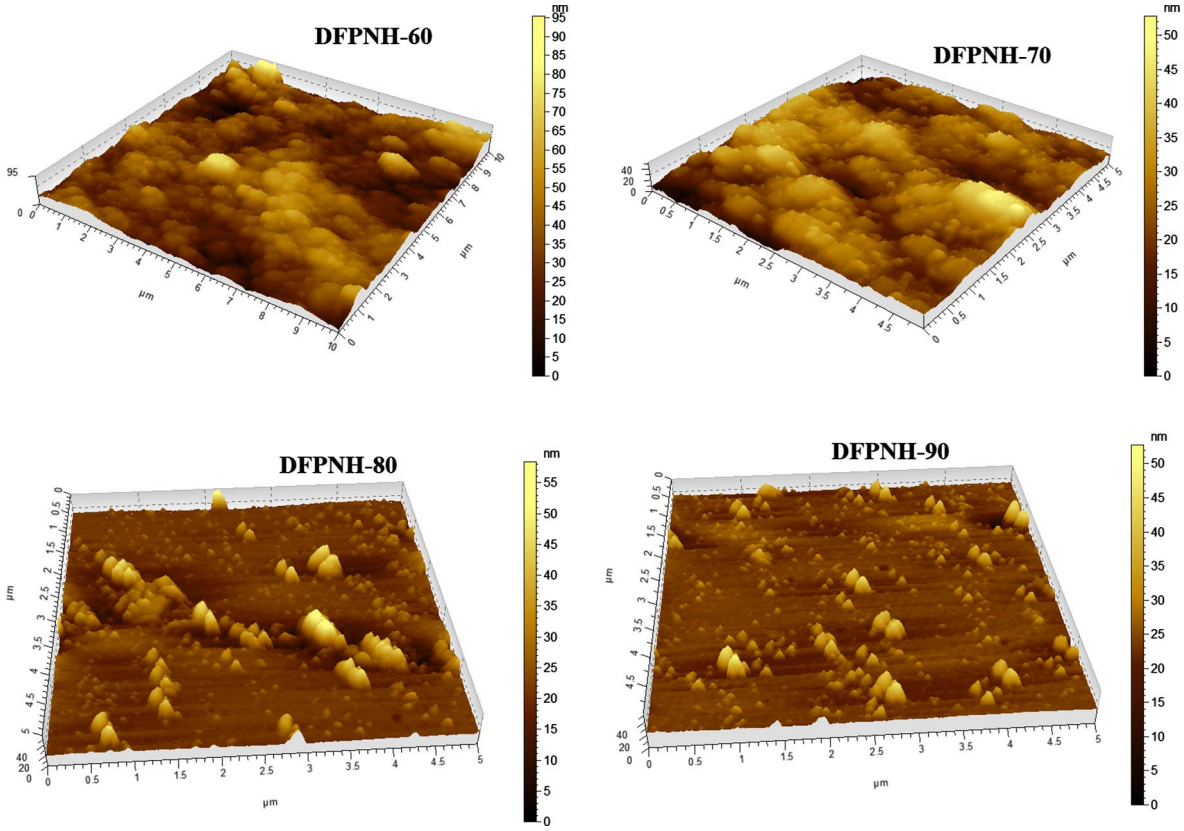

Fig. 8. 3D tapping mode AFM images of the DFPNH-XX copolymer membranes.

matrix).

For further rationalization of the bulk morphology of all the copolymer membranes, transmission electron microscopy (TEM) has also been performed. The TEM micrographs (cross section) of the co-SPI membranes showed excellent nano-phase separated morphology (Fig. 9). The black spherical region corresponds to the hydrophilic sulfonic acid groups and the bright region corresponds to the hydrophobic region in the polymer backbone. With the increase in DS of the co-SPI membranes (DFPNH-80 and DFPNH-90), the size and number density of the hydrophilic clusters were increases. The higher conductivity of these copolymers can be attributed to the good hydrophilic/hydrophobic phase separation and closer proximity of hydrophilic clusters domains with interconnected ionic channels [15,23,32].

3.6. Proton conductivity

In plane proton conductivities of DFPNH-XX membranes were measured as a function of temperature (in the range 30–90 °C) in water using AC impedance spectroscopy. The proton conductivity values of the membranes were found in the range 16 to 111 mS cm^{-1} at 30 °C and 33 to 261 mS cm^{-1} at 90 °C (Table 5). The proton conductivity of the co-SPIs increases with increase in temperature and DS values. The proton conductivity of the synthesized co-SPIs was higher than many other SPIs (comparable IEC_w) under similar experimental conditions [24]. The higher proton conductivity of DFPNH-70 than p-DTN-70 (comparable IEC_w) was attributed to the presence of phosphine oxide moiety in DFPNH-70 which forms hydrogen bonding with the sulfonic acid present in the polymer and facilitate proton transport. However, the proton conductivity of the DFPNH-60 was found to be lower than the previously reported analogous copolymer TPPO-60 with the same DS value (Table 5) [23]. This can be related to the lower IECw value of DFPNH-60 compared to TPPO-60. However, the fluorinated DFPPO monomer allows to prepare the copolymers (due to the higher solubility of the copolymers) with higher DS values (XX = 70, 80, 90) that eventually increases the IEC and proton conductivity values.

The proton conductivity values of all the membranes increase with increase in temperature due to the more effective movement of protons [33]. The proton conductivity of the membranes was plotted against 1/T that showed Arrhenius-type temperature dependence as shown in Fig. 10. The activation energy (E_a) of the proton conductivity for the co-SPI membranes was calculated from the slope of the lines, using a linear least square fit. The E_a values for the polymers are tabulated in Table 5 and were found within the range of 12.6 to 14.9 kJ mol^{-1}, which are comparable to Nafion® 117. This further explains the usefulness of these polymer for PEM application.

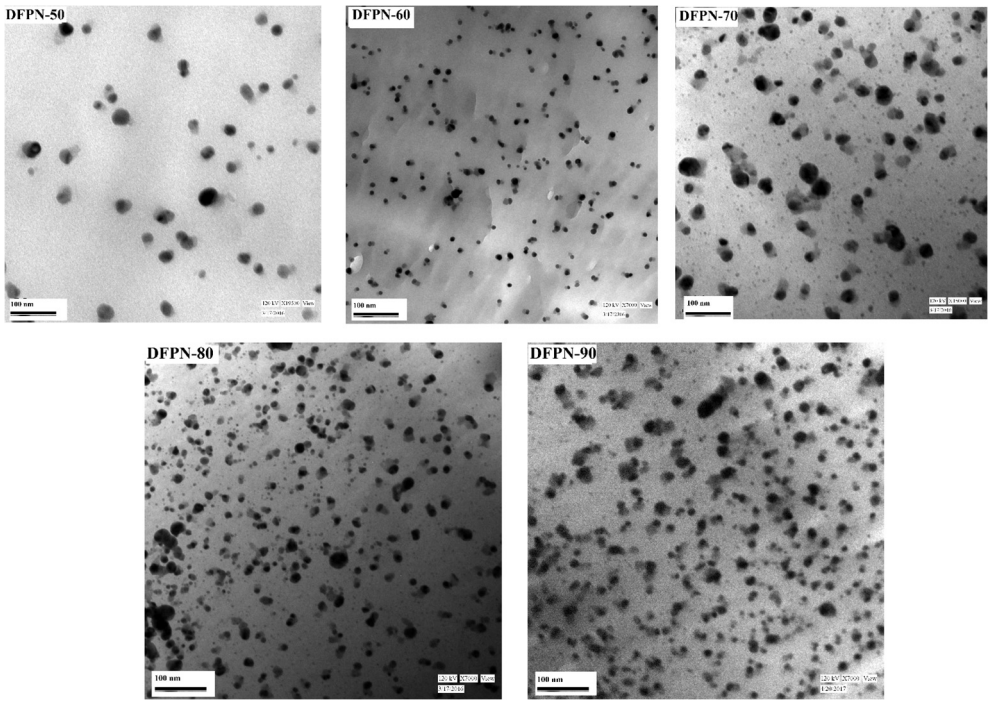

Fig. 9. TEM images of silver ion-stained DFPNH-XX copolymer membranes.

Table 5
Proton conductivity of the DFPNH-XX membranes.

Polymers	IEC_w (mequiv g^{-1})	Proton conductivity[a] (mS cm^{-1})			E_a kJ/mol
		30 °C	80 °C	90 °C	
DFPNH-50	1.36	16	33	36	12.6
DFPNH-60	1.70	35	81	94	14.9
DFPNH-70	2.05	66	142	162	13.9
DFPNH-80	2.44	82	181	207	13.8
DFPNH-90	2.86	111	237	261	13.2
p-DTN-70[b]	2.1	24	45	53	–
TPPO-60[c]	1.84	46	99	107	12.3
Nafion® 117	0.90	90	165	–	13.6

[a] Measured in water.
[b] Reference [24].
[c] Reference.[23].

4. Conclusion

A new trifluromethyl substituted phosphine oxide containing diamine monomer was designed and prepared. The monomer was deployed along with DSDSA to prepare a series of sulfonated co-SPIs (DFPNH-XX) with a controlled degree of sulfonation on reaction with NDTA. All these copolymers showed good solubility in many common organic solvents attributed to the presence of non-coplanar phosphine oxide moieties, pendant trifluoro methyl groups and ether linkages in the polymer structures which helped in disrupting the chain regularity. Because of higher solubility of these copolymers in polymerization solvent, it was possible to prepare copolymers with a higher degree of sulfonation. Different NMR techniques were used for detailed structural elucidation of the copolymers. The degree of sulfonation of the copolymers was calculated from the polymer composition determined by ^{1}H NMR spectroscopy. Thermally and mechanically stable membranes were prepared from these copolymers through solution casting route and their different PEM properties were studied. In general, all the polymers showed better water management, higher oxidative stability and higher proton conductivity than many other sulfonated polyimides reported earlier. The proton conductivity values were in the range of 16–111 mS/cm at 30 °C, 36–261 mS/cm at 90 °C. Notably, the copolymer DFPNH-70 (DS = 70) showed a proton conductivity as high as 142 mS/cm at 80 °C (Nafion® 117–165 ms/cm) and an interesting set of other PEM properties for a practical application. TEM analysis showed well separated morphology of the hydrophilic and hydrophobic domains that were responsible for high proton conductivity. It can be deduced that the presence of both phosphine oxide moieties and the trifluromethyl groups has a

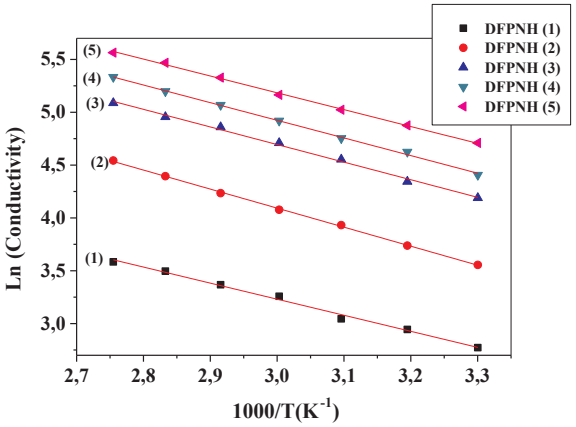

Fig. 10. Temperature dependent proton conductivity of DFPNH-XX copolymer membranes.

synergistic effect towards membrane properties for PEM application. Finally, we can state that we have been able to make a new series of sulfonated copolymers that have all potential to be used in future PEM application.

Acknowledgements

AKM thanks CSIR, New Delhi, for providing a fellowship to carry out this research. Ch. Harnisch (Leibniz-Institut für Polymerforschung Dresden e. V.) is acknowledged for SEC measurements.

References

[1] M.A. Hickner, H. Ghassemi, Y.S. Kim, B.R. Einsla, J.E. McGrath, Alternative polymer systems for proton exchange membranes (PEMs), Chem. Rev. 104 (2004) 4587–4612.
[2] H. Zhang, P.K. Shen, Recent development of polymer electrolyte membranes for fuel cells, Chem. Rev. 112 (2012) 2780–2832.
[3] R. Devanathan, Recents developments in proton exchange for fuel cells, Energy Environ. Sci. 1 (2008) 101–119.
[4] S. Bose, T. Kuila, T.X.H. Nguyen, N.H. Kim, K. Lau, J.H. Lee, Polymer membranes for high temperature proton exchange membrane fuel cell: Recent advances and challenges, Prog. Polym. Sci. 36 (2011) 813–843.
[5] C.H. Park, C.H. Lee, M.D. Guiver, Y.M. Lee, Sulfonated hydrocarbon membranes for medium-temperature and low-humidity proton exchange membrane fuel cells (PEMFCs), Prog. Polym. Sci. 36 (2011) 1443–1498.
[6] W.L. Harrison, F. Wang, J.B. Mecham, V.A. Bhanu, M. Hill, Y.S. Kim, J.E. Mcgrath, Influence of the bisphenol structure on the direct synthesis of sulfonated poly (arylene ether) copolymers. I, J. Polym. Sci, Part A, Polym. Chem. 41 (2003) 2264–2276.
[7] E.A. Mistri, A.K. Mohanty, S. Banerjee, H. Komber, B. Voit, Naphthalene dianhydride based semifluorinated sulfonated copoly(etherimide)s: synthesis, characterization and proton exchange properties, J. Membr. Sci. 441 (2013) 168–177.
[8] J. Fang, X. Guo, H. Xu, K. Okamoto, Sulfonated polyimides: Synthesis, proton conductivity and water stability, J. Power Sources 159 (2006) 4–11.
[9] Y. Yin, Q. Du, Y. Qin, Y. Zhou, K. Okamoto, Sulfonated polyimides with flexible aliphatic side chains for polymer electrolyte fuel cells, J. Membr. Sci. 367 (2011) 211–219.
[10] R. Mukherjee, A.K. Mohanty, S. Banerjee, H. Komber, B. Voit, Phthalimidine based fluorinated sulfonated poly(arylene ether sulfone) s copolymer proton exchange membranes, J. Membr. Sci. 435 (2013) 145–154.
[11] R. Mukherjee, S. Banerjee, H. Komber, B. Voit, Highly proton conducting fluorinated sulfonated poly(arelene ether sulfone) copolymers with side chain grafting, RSC Adv. 4 (2014) 46723–46736.
[12] A. Singh, R. Mukherjee, S. Banerjee, H. Komber, B. Voit, Sulfonated polytriazoles from a new fluorinated diazide monomer and investigation of their proton exchange properties, J. Membr. Sci. 469 (2014) 225–237.
[13] K.Y. Amazaki, H. Kawakami, High proton conductive and low gas permeable sulfonated graft copolyimide membrane, Macromolecules 43 (2010) 7185–7191.
[14] C. Liu, L. Li, Z. Liu, M. Guo, L. Jing, B. Liu, Z. Jiang, T. Matsumoto, M.D. Guiver, Sufonated naphthalenic polyimides containing ether and ketone linkages as polymer electrolyte membranes, J. Membr. Sci. 366 (2011) 73–81.
[15] E.A. Mistri, A.K. Mohanty, S. Banerjee, Synthesis and characterization of new fluorinated poly(ether imide) copolymers with controlled degree of sulfonation for proton exchange membranes, J. Membr. Sci. 411–412 (2012) 117–129.
[16] B.R. Einsla, Y.T. Hong, Y.S. Kim, F. Wang, N. Gunduz, J.E. McGrath, Sufonated naphthalene dianhydride based polyimide copolymers for proton exchange membrane fuel cells. I. Monomer and copolymer synthesis, J. Polym. Sci, Part A Polym. Chem. 42 (2004) 862–874.
[17] J. Miyake, M. Watanabe, K. Miyatake, Sulfonated poly (arylene ether phosphine oxide ketone) block copolymers as oxidatively stable proton conductive membranes, ACS Appl. Mater. Interfaces 5 (2013) 5903–5907.
[18] D.W. Shin, S.Y. Lee, N.R. Kang, K.H. Lee, M.D. Guiver, Y.M. Lee, Durable sulfonated poly(arylene sulfide sulfone nitrile)s containing naphthalene units for direct methanol fuel cells (DMFCs), Macromolecules 46 (2013) 3452–3460.
[19] S. Banerjee, A. Ghosh, Semifluorinated Aromatic Polymers and Their Properties, In: Fluorinated Polymers: Volume 1: Synthesis, Properties, Processing and Simulation, Ed. B. Ameduri and H. Sawada, The Royal Society of Chemistry, Chapter 5, (201) 103-188.
[20] A. Ghosh, S. Banerjee, Sulfonated fluorinated-aromatic polymers as proton exchange membranes, e-Polymer 14 (2014) 227–257.
[21] S. Banerjee, Handbook of Specialty Fluorinated Polymers: Preparation, Properties, and Applications, Elsevier, 2015.
[22] A. Kraytsberg, Y. Ein-eli, Review of advanced materials for proton exchange membrane fuel cells, Energy Fuels 28 (2014) 7303–7330.
[23] A.K. Mandal, D. Bera, S. Banerjee, Sulfonated polyimides containing triphenylphosphine oxide for proton exchange membranes, Mater. Chem. Phys. 181 (2016) 265–276.
[24] E.A. Mistri, S. Banerjee, H. Komber, B. Voit, Structure–property correlation of semifluorinated 6-membered co-SPIs for proton exchange membrane, Eur. Polym. J. 7 (2015) 466–479.
[25] H. Satpathi, D. Pospiech, S. Banerjee, B. Voit, Decomposition and combustion studies of phosphine oxide containing aromatic polyethers, Polym. Degrad. Stab. 107 (2014) 53–63.

[26] H. Bai, W.S.W. Ho, Newpoly(ethyleneoxide) soft segment containing sulfonated polyimide copolymers for high temperature proton exchange membrane fuel cells, J. Membr. Sci. 313 (2008) 75–85.
[27] M.F.H. Schuster, W.H. Meyer, M. Schuster, K.D. Kreuer, Toward a new type of anhydrous organic proton conductor based on immobilized imidazole, Chem. Mater. 16 (2004) 329–337.
[28] S. Adanur, H. Zheng, Synthesis and characterization of sulfonated polyimide based membranes for proton exchange membrane fuel cells, J. Fuel Cell Sci. Technol. 10 (2013) 041001–041005.
[29] Y.S. Kim, B.S. Pivovar, Moving beyond mass-based parameters for conductivity analysis of sulfonated polymers, Annu. Rev. Chem. Biomol. 1 (2010) 123–148.
[30] N. Asano, M. Aoki, S. Suzuki, K. Miyatake, H. Uchida, M. Watanabe, Aliphatic/Aromatic polyimide ionomers as a proton conductive membrane for fuel cell applications, J. Am. Chem. Soc. 128 (2006) 1762–1769.
[31] A. Ganeshkumar, D. Bera, E.A. Mistri, S. Banerjee, Triphenyl amine containing sulfonated aromatic polyimide proton exchange membranes, Eur. Polym. J. 60 (2014) 235–246.
[32] N. Li, M.D. Guiver, Ion transport by nanochannels in ion-containing aromatic copolymers, Macromolecules 47 (2014) 2175–2198.
[33] C. Wang, N. Li, D.W. Shin, S.Y. Lee, N.R. Kang, Y.M. Lee, M.D. Guiver, Macromolecules 44 (2011) 7296–7306.